

# GFD 2006 Lecture 9: Thermomolecular flow, thermal regelation and frost heave

Grae Worster; notes by Takahide Okabe and Dan Goldberg

30 June, 2006

## 1 Review

In the last lecture, interactions that cause macroscopic disjoining pressure between two materials separated by a third material were discussed. Microscopically, that disjoining pressure may be due to non retarded Van der Waals forces, or may be due to retarded Van der Waals forces, or to electrostatic forces. But the main results discussed below are independent of the microscopic theory. As we will see, everything boils down to the Generalized Clapeyron equation, which is derived from the Gibbs-Duhem relation and gives the difference in pressure between solid and liquid phases of the same material.

### Marangoni flow vs. thermomolecular flow

Let us review the discussion of the last lecture in pictures. We compared Marangoni flows (Figure 1) with thermomolecular flows (Figure 2). Marangoni flows are driven by gradients of the surface tension at the fluid interface, between liquid and vapor, for example. The temperature gradient gives the gradient of the surface tension: surface tension is low at the warm end, and high at the cold end. That provides the surface traction on the film that pulls the surface water to the right, building up the liquid pressure on the right due to curvature, which can drive the bottom water to the left. Thus, it is possible to achieve steady state in this way. By contrast, in thermomolecular flows, the driving force is differential normal stresses. The temperature gradient gives the gradient of the thermomolecular pressure: thermomolecular pressure is low at the warm end and high at the cold end. Therefore hydrodynamic pressure is high at the warm end and low at the cold end in order to balance the solid pressure. That causes flow from the warm end to the cold. This distinction between Marangoni flows and thermomolecular flows is the distinction between being driven by tangential stress or normal stress, and in the thermomolecular case, film thickness is determined only by the temperature field, whereas, in Marangoni flow, it is determined dynamically as water moves from one end to another. But tangential stress as a driver goes away if vapor is replaced by solid, and we have only to consider thermomolecular flows. We concentrate on this situation in today's lecture.

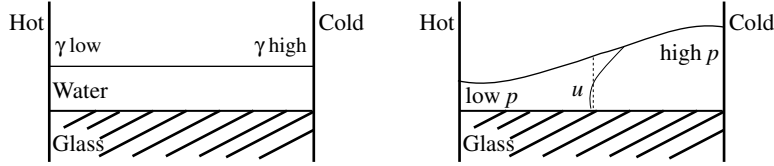


Figure 1: Marangoni flow. Initially, water is level on the glass, but if the temperature gradient is given externally, it causes the difference in surface tension. This results in the flow of surface water, and water is built up on the right. Then the pressure at the bottom is higher at the cold end, which causes the flow of the bottom water to the left.

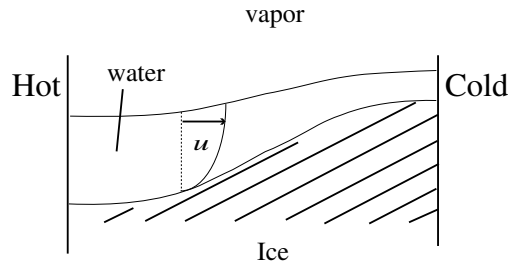


Figure 2: Since water is on ice, thermomolecular pressure plays an important role. Thermomolecular pressure is determined by temperature: low at the hot end and high at the cold end. Since thermomolecular pressure plus liquid pressure is equal to solid pressure, liquid pressure is high at the hot end and low at the cold end, which causes the flow to the cold end.

## 2 Premelted Film in a Capillary Tube

Let us consider the following thought experiment. Imagine we have a capillary tube, which is filled with water, with one end colder than  $T_m$ . Since the left end is below the freezing temperature, then there is ice on the left and water on the right. This is a classical Stefan problem with fixed temperature field varying from cold to warm. As we saw in the previous lecture, the interface between ice and water simply stops when it reaches the position at which  $T = T_m$ . Now imagine this is a real capillary tube: we need to take into account interactions between the material of the wall of the tube and the ice, which in principle can cause the ice to be premelted, producing a thin layer of water next to the wall. Because the left side is colder, we have relatively large disjoining pressure and low liquid pressure on the left. This pressure gradient has a tendency to move fluid from warm to cold. If this is a theoretician's ideal rigid capillary tube, nothing more happens: the differential stress is accommodated by the wall (Figure 3). However if this wall is elastic, then the water in the premelted film can flow. This situation is depicted in Figure 4. We will make a particular assumption about the elastic tube: that it just exerts a hoop stress (circumferential stress), not taking account of any bending moment of the wall.

The film is thick where it is warm and thinner where it is cold. We are going to take a

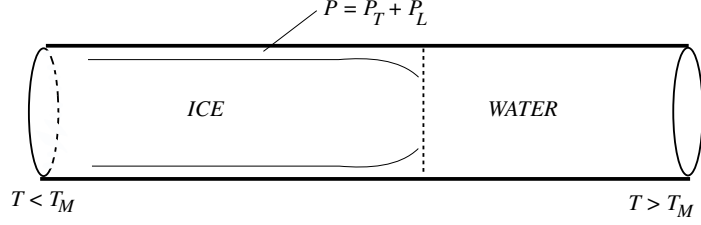


Figure 3: Rigid capillary tube

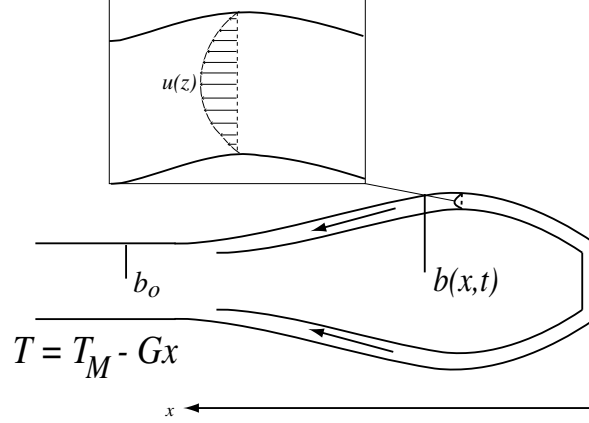


Figure 4: Elastic capillary tube

1-dimensional coordinate system  $x$  as depicted in Figure 4. Then the temperature field is  $T = T_m - Gx$ . Let the radius of the capillary be  $b(x, t)$ . Because we treat the elastic hoop stress only, the pressure of the wall is equal to the pressure of the solid:

$$p_w = p_s = k(b - b_0), \quad (1)$$

$$p_l = p_s - p_T = k(b - b_0) - \frac{\rho_s L}{T_m} (T_m - T). \quad (2)$$

Where the temperature is colder,  $T_m - T$  is larger and the liquid pressure is lower. Liquid pressure is decreasing in the positive  $x$ -direction, and this pushes fluid in the direction toward the cold end. The premelted film has thickness  $d$  given by

$$\rho_s L \frac{T_m - T}{T_m} = \frac{A}{6\pi d^3}. \quad (3)$$

Because the temperature field is stationary, the film thickness  $d$  is also independent of time. Later, we will consider how to modify the formulation in the presence of a curved solid–liquid interface. For the moment, we ignore this curvature. Lubrication theory gives volume flow rate (in 2D)

$$q = \frac{d^3}{12\mu} \left( -\frac{\partial p_l}{\partial x} \right). \quad (4)$$

Conservation of mass gives

$$\frac{\partial b}{\partial t} + \frac{\partial q}{\partial x} = 0 \quad (5)$$

$$\Rightarrow \frac{\partial b}{\partial t} = \frac{\partial}{\partial x} \left[ \frac{d^3}{12\mu} \frac{\partial p_l}{\partial x} \right] \quad (6)$$

$$= \frac{\partial}{\partial x} \left[ \frac{AT_m}{6\pi\rho_s L} \frac{1}{Gx} \frac{1}{12\mu} \left( k \frac{\partial b}{\partial x} - \frac{\rho_s L}{T_m} G \right) \right]. \quad (7)$$

Therefore

$$\frac{\partial b}{\partial t} = \frac{AT_mk}{72\pi\mu\rho_s LG} \frac{\partial}{\partial x} \left[ \frac{1}{x} \left( \frac{\partial b}{\partial x} - \frac{\rho_s LG}{kT_m} \right) \right]. \quad (8)$$

This can be regarded as a modified diffusion equation with spatially varying diffusivity. There is a similarity solution to (8). By using the following variables

$$b - b_0 = \frac{\rho_s LG}{T_m k} \left( \frac{k\Gamma^3 t}{12\mu G} \right)^{\frac{1}{3}} g(\eta) \quad (9)$$

where

$$d = \Gamma(T - T_m)^{-\frac{1}{3}}, \quad (10)$$

$$\Gamma = \left( \frac{AT_m}{6\pi\rho_s L} \right)^{\frac{1}{3}}, \quad (11)$$

$$\eta = \left( \frac{12\mu G}{k\Gamma^3} \right)^{\frac{1}{3}} \frac{x}{t^{\frac{1}{3}}}, \quad (12)$$

(8) becomes dimensionless:

$$g'' = \frac{-1 + g'}{\eta} + \frac{1}{3}\eta g - \frac{1}{3}\eta^2 g' \quad (13)$$

with boundary conditions

$$g = 0 \quad (\eta = 0), \quad (14)$$

$$g \rightarrow 0 \quad (\eta \rightarrow \infty). \quad (15)$$

where  $g$  is the dimensionless displacement. The displacement is 0 at the end, because there is no force there (we are only considering the hoop stress. If we were considering curvature stress as well, it would be nonzero.) The displacement is increasing in time. The tube expands at first, but eventually stops expanding, because the elastic hoop stress which pushes back on the ice balances with the thermomolecular pressure pushing out. If we leave it for infinitely long time, we get a linear deformation profile, matching the linear temperature profile.

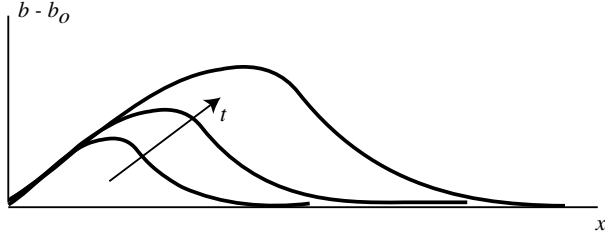


Figure 5: Similarity solution. Typical values for  $b - b_0$  are  $\sim 1\mu\text{m}$  when  $x \sim 100\mu\text{m}$ . Corresponding timescales are on the order of several days.

### 3 Thermal Regelation

Imagine there is a big block of ice containing an immersed solid particle. We impose a temperature gradient  $\nabla T = \mathbf{G}$  such that the temperature is everywhere below the bulk freezing point. There is a premelted film against the object which is thinner where the temperature is lower (Figure 6). The thermomolecular force of the film is greater where it is thinner, so there is a net force on the particle, pushing the particle downwards. Movement of the particle can take place by the melting of ice on one side and freezing on the other, a process known as *regelation*. In order for regelation to take place, liquid must be transported within the film from the melting front to the freezing front. And in general the particle migrates from cold region to warm region. We want to understand how to calculate this phenomenon.

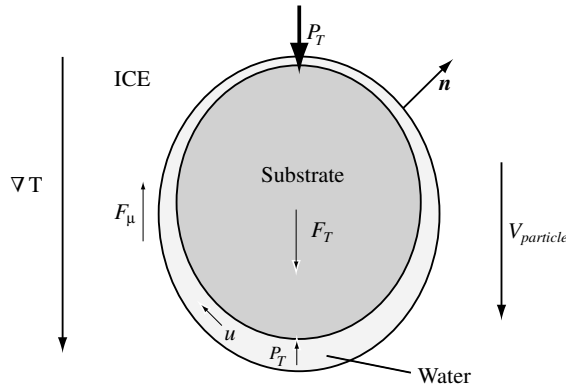


Figure 6: Solid particle in ice

For small particles, premelting is affected by curvature of the solid-liquid interface:

$$p_s = p_l + p_T + \gamma_{sl} \nabla \cdot \mathbf{n} \quad (16)$$

where  $p_s$  is solid pressure,  $p_l$  is liquid pressure,  $p_T$  is the pressure due to disjoining force. The unit normal  $\mathbf{n}$  points into the ice. The last term is a pressure due to curvature of the

interface. We need to take the Generalized Clapeyron equation into account:

$$\rho_s L \frac{T_m - T}{T_m} = p_s - p_l \quad (17)$$

$$= \frac{A}{6\pi d^3} + \gamma_{sl} \nabla \cdot \mathbf{n}. \quad (18)$$

Because (total force on the particle) = -(total force on the ice),

$$\mathbf{F} = - \int_{\partial \mathcal{D}} p_s (-\mathbf{n}) dS \quad (19)$$

$$= \int_{\partial \mathcal{D}} p_l \mathbf{n} dS + \int_{\partial \mathcal{D}} \rho_s L \frac{T_m - T}{T_m} \mathbf{n} dS \quad (20)$$

$$= \mathbf{F}_\mu + \mathbf{F}_T \quad (21)$$

where  $\mathcal{D}$  is the whole region that is not occupied by ice.  $F_\mu$  is due to lubrication pressure and  $F_T$  is the thermomolecular force.

$$\mathbf{F}_T = \int_{\partial \mathcal{D}} \rho_s L \frac{T_m - T}{T_m} \mathbf{n} dS = \frac{\rho_s L}{T_m} \int_{\mathcal{D}} \nabla T dV. \quad (22)$$

If the thermal properties of all phases are the same, then  $\nabla T = \mathbf{G}$  throughout. Under this assumption,

$$\mathbf{F}_T = \frac{\rho_s L}{T_m} \mathbf{G} \cdot (\text{volume that is not ice}) \quad (23)$$

$$= \frac{L}{T_m} \mathbf{G} \cdot (\text{mass of displaced ice}). \quad (24)$$

This looks similar to the principle of Archimedes, which states that the upthrust on a body immersed in water is proportional to the mass of water displaced. This motivates the term “thermodynamic buoyancy” to describe the total thermomolecular force on an immersed particle. The result is independent of the particular intermolecular interactions that underly the thermomolecular pressure.

To find the regelation velocity,  $\mathbf{F}_\mu$  must also be dealt with, generally using lubrication theory, or some closure such as Darcy’s Law. In the next section this is done in investigating the phenomenon of frost heave.

## 4 Frost Heave

Frost heave is a phenomenon that involves upheaval of soil from formation of ice within the soil, and is known in some cases to cause the formation of “lenses” - layers of ice containing little or no soil particles (figure 7).

Frost heave is essentially the process of thermal regelation on a large scale in frozen soil. There is an external temperature gradient that leads to a thermomolecular force on the soil particles, as in the previous example of regelation, and that balances the viscous forces from the transport of water necessary for the regelation.

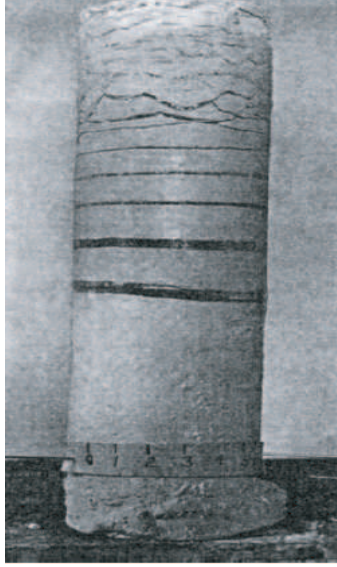


Figure 7: A column of frozen soil in which lenses (dark) have formed in between layers of frozen soil (light). From Taber (1929).

In the model presented here, the temperature gradient is assumed to be constant and directed downwards, so at some depth ( $z = 0$ ) the temperature is at the bulk freezing point. However, the soil is not frozen all the way down to  $z = 0$ ; the ice formed in the soil pores has an associated curvature because of the geometry of the pores, and so the Gibbs-Thomson effect prohibits ice formation at temperatures below the freezing point. And so there is a *fringe* region of frozen soil with lower boundary  $z_f > 0$  and upper boundary  $z_l$  (the lens boundary).  $z_f$  is set by the geometry of the soil, so if  $z_l < z_f$ , there is no fringe region. Figure 8 shows the situation where there is a fringe.

First assume that a fringe does exist. A force balance on the fringe section can be calculated, as long as certain properties of the ice-soil system (e.g. volume fraction, permeability) are known. The total upward thermomolecular force  $F_T$  is equal to the thermomolecular pressure integrated over the substrate surface:

$$F_T = \hat{\mathbf{z}} \cdot \int_{\Gamma} p_T \mathbf{n} \, d\Gamma = \hat{\mathbf{z}} \cdot \frac{\rho_s L G}{T_m} \int_{\Gamma} z \mathbf{n} \, d\Gamma, \quad (25)$$

where  $G = |\nabla T|$  and  $\Gamma$  is the surface of the ice. The divergence theorem lets us write

$$F_T = \frac{\rho_s L G}{T_m} \int_0^{z_l} (1 - \phi) dz, \quad (26)$$

where  $\phi$  is the volume fraction of ice in the soil, assumed to be only a function of  $z$ . Also acting on the mass of ice is the hydrodynamic pressure necessary to bring water to the freezing front (or take water away from the melting front). We can use Darcy's Law to infer the relation between pressure and pore transport, and we can use continuity to find the magnitude of this transport:

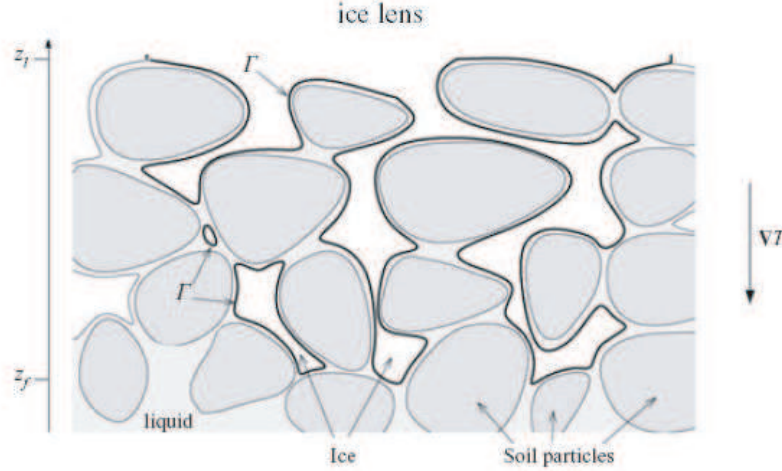


Figure 8: Cross section through the fringe region.  $z_f$  and  $z_l$  mark the lower and upper boundaries of the fringe.  $\Gamma$  is the ice boundary, with unit normal pointing into the ice, as in the previous regelation example. From Rempel *et al* (2004).

$$W = (1 - \phi)V_h \quad (27)$$

and

$$\mu W = -\Pi(\phi)\nabla p_L. \quad (28)$$

Here  $W$  is the area-averaged vertical water transport,  $V_h$  is the heave velocity,  $p_L$  is the hydrodynamic water pressure driving the flow, and  $\Pi$  is the permeability of the soil.  $\Pi$  is, in general, dependent on many factors, including soil particle geometry. However, it is written as a function of ice volume fraction only to emphasize the fact that permeability decreases as ice volume fraction increases. So if  $\phi(z)$  and  $\Pi(\phi)$  are known functions, we can calculate the hydrodynamic force acting on the fringe section:

$$\begin{aligned} F_\mu &= \hat{\mathbf{z}} \cdot \int_\Gamma p_L \mathbf{n} d\Gamma \\ &= - \int_{z_h}^{z_l} \frac{\partial p}{\partial z} (1 - \phi) dz \\ &= \mu V_h \int_{z_h}^{z_l} \frac{(1 - \phi)^2}{\Pi(\phi)} dz. \end{aligned} \quad (29)$$

$z_h$  is a reference point below the fringe where  $p_L$  goes to zero. The choice of  $z_h$  is somewhat arbitrary, but the result above is not likely to be sensitive to  $z_h$  as most of the pressure drop occurs near  $z_l$ , where permeability is greatly reduced due to the high ice concentration.

Before proceeding, note that the above analysis also applies when  $z_l < z_f$ , i.e. there is no frozen fringe. The expression for  $F_T$ , for example, reduces to  $\rho_s L (T_m - T(z_l)) T_m^{-1}$ , the expression for the thermomolecular force at the temperature at the lens boundary.



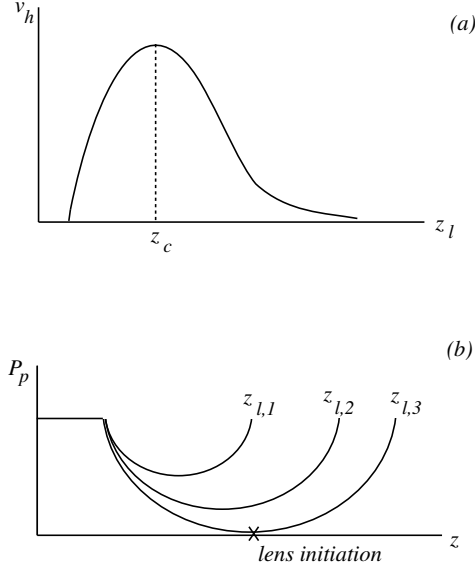


Figure 9: (a) Frost heave rate as a function on  $z_l$  (in the domain where freezing occurs). (b) Soil particle effective stress as a function of depth for different lens heights.

The only other force acting on the mass of ice is the weight above it,  $P_0$ . Solving for  $V_h$  gives

$$V_h = \left[ \frac{\rho_s LG}{T_m} \int_0^{z_l} (1 - \phi) dz - P_0 \right] \left[ \mu \int_{z_h}^{z_l} \frac{(1 - \phi)^2}{\Pi(\phi)} dz \right]^{-1}. \quad (30)$$

In general, the vertical distribution of  $\phi$  and the associated permeability dependence must be known or calculated. Rempel *et al* (2004) use an idealized model for ice saturation and permeability dependence, but certain properties of the dependence of  $V_h$  on  $z_l$  can be deduced for more general cases. For instance, the thermomolecular force ( $\rho_s LG \int_0^{z_l} (1 - \phi) dz / T_m$ ) is monotonic in  $z_l$ , and so the heave velocity is zero for a certain value  $z_l$  and positive for higher values. Further, we expect the permeability will tend to zero as the ice fraction goes to 1, so we expect that the denominator of ((30) becomes large with large  $z_l$ , and so  $V_h$  tends to zero. We can then expect that  $V_h$  goes through a maximum at some point. Rempel *et al* find a curve similar to that shown in figure 9(a) for the heave rate.

The frost heave phenomenon can be demonstrated in a lab setting. A column of frozen soil with a lens is placed longitudinally in a temperature gradient that is fixed (w.r.t. the lab frame) as in figure 10. The entire column can be moved at constant velocity through the gradient. Meanwhile, the lens position can move relative to the moving frame due to frost heave. A steady state can be found in which the lens does not move relative to the lab frame. One can view the setup as the lens being pulled through the soil, which remains in place as the liquid flows through it, providing the hydrodynamic force that balances the thermomolecular force.

From figure 9(a) it is obvious that for a range of  $V$  (the rate at which the column in

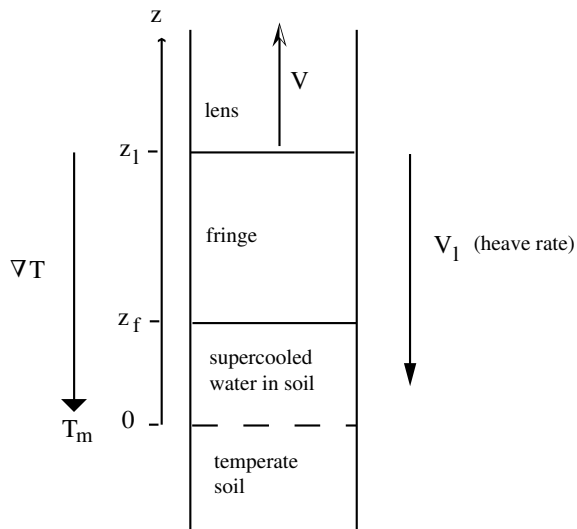


Figure 10: The experiment described in Rempel *et al.* The entire system is pulled upward, while positive heave rates push the soil in the opposite direction.

the experiment is moved through the temperature gradient) there are 2 steady heave rates. However, only one state (the one with  $z_l < z_c$ ) is stable to small perturbations; if  $V_h(z_l)$  is sloping downwards, then a small increase in  $z_l$  will slow the heave rate, and the lens front will move forward (increasing  $z$ ). Physically, a decrease in permeability limits the amount of liquid that can be brought to the front. The situation is similar for small decreases in  $z_l$ .

## Lens Initiation

One might ask how a lens will form initially. To determine where this might occur, the vertical force between soil particles ( $F_p$ ) is examined. At each point,  $F_p$  balances the sum of the overburden, the thermomolecular force, and the hydrodynamic force. Thus  $p_p$  (inter-particle force per unit area) can be calculated from

$$F_p(z) = V_h \mu \int_{z_h}^z \frac{(1 - \phi)^2}{\Pi(\phi)} dz + P_0 - \frac{\rho_s LG}{T_m} \left[ \int_0^z (1 - \phi) dz - z(1 - \phi(z)) \right]. \quad (31)$$

Note the similarity to (30) with  $z_l$  replaced by  $z$ . The last term,  $\rho_s LGz(1 - \phi(z))/T_m$ , can be seen as the additional force that would act on the volume of integration (that is, a volume similar to that bounded by  $\Gamma$  in figure(8)) were the ice fraction at  $z$  equal to unity. If  $p_p$  becomes zero at some point, there is virtually nothing holding the soil particles together, and a lens has the potential to form.

Again, this expression depends on the specific forms of  $\phi$  and  $\Pi(\phi)$ . For the idealized configuration mentioned above, Rempel *et al* calculated  $p_p(z)$  for different values of  $z_l$ , and found that the minimum  $p_p$  decreases with increasing  $z_l$ , and at some point  $p_p(z)$  becomes zero at a height less than  $z_l$  (figure 9(b)). If a lens were to form at this height, then  $z_l$  would be effectively decreased. One can imagine a situation, such as in the lab experiment

described above, in which the lens front is continually moving upward, with new lenses periodically forming below the previous lens front. Such a phenomenon has in fact been observed in the laboratory, and is believed to be responsible for similar patterns that are formed in situ (figure 7).

## References

- [1] Rempel, A.W., Wettlaufer, J.S. & Worster, M.G. 2004. Premelting Dynamics in a Continuum Model of Frost Heave. *J. Fluid Mech.*, **498**, 227-244.
- [2] Taber, S. 1929. Frost heaving. *J. Geol.*, 37, 428-461.